Optica Applicata, Vol. XXXVIII, No. 2, 2008

Thermal parameters of solids determination by the photodeflection method – theories and experiment comparison

DOROTA KORTE KOBYLIŃSKA*, ROMAN J. BUKOWSKI,
JERZY BODZENTA, STANISŁAW KOCHOWSKI

Institute of Physics, Silesian University of Technology, ul. Bolesława Krzywoustego 2,
44-100 Gliwice, Poland

*Corresponding author: dkorte@polsl.pl

This paper is concerned with the application of complex geometrical optics equations to sample thermal parameters determination by the photodeflection method. The thermal diffusivity of a sample is determined using the four parameters least-squares-fitting of theoretical dependence of normal photodeflection signal on angular modulation frequency to the experimental data. The calculation of the signal on the basis of complex geometrical optics is proved to be more accurate approach of determining the sample thermal diffusivity than that based on the geometrical and wave optics.

Keywords: photodeflection method, mirage effect, complex geometrical optics, sample thermal parameters determination.

1. Introduction

The necessity of applying new materials in modern technology demands their testing and characterization [1, 2]. One of the techniques used for determining the thermal diffusivity of a wide range of specimens is the photodeflection method. In the simplified version of this method, a modulated light beam of angular frequency Ω (the pump beam) illuminates the sample surface uniformly, and another laser beam (the probe beam) is used for detecting, through the optical beam deflection effect, the produced thermal gradients (the thermal lens) (Fig. 1).

The interpretation of the photodeflection signal may cause problems, especially when studying small objects and thin films in case of which it is necessary to use high frequency of thermal waves. The well-known geometrical optics model (GOM)

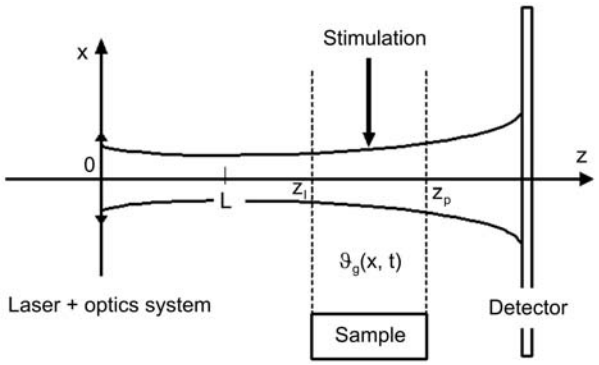

Fig. 1. Schematic diagram of the photodeflection setup in the *mirage* effect geometry.

of describing the photodeflection signal [3, 4] is usually limited by frequency of several kilohertz and is based on the assumption that the probe beam is a bundle of rays. Each of them is deflected in the thermally disturbed medium. Their contribution to the photodeflection signal is averaged in accordance with the probe beam intensity distribution in the temperature field vicinity. Another approach [2, 5–7] is the wave optics model (WOM) which describes the mirage effect by the use of the diffraction theory. According to it, the field of thermal wave is considered to be a phase lens. This means that only the phase changes in the electric field of the probe beam caused by the temperature field are taken into account. Their influence on the amplitude distribution of the probe beam is neglected. Such an approach can be used for thermal parameters determination in a wider frequency range of thermal waves. We should use it with care because this model still does not describe all the effects of probe beam interaction with the field of thermal waves and for some parameters of the experimental setup its agreement with experiment is not satisfying [8].

It was proved in [8, 9] that the method of calculating the photodeflection signal based on the complex geometrical optics equations (the complex ray model, CRM [8–13]) is a more accurate approach in comparison with those used so far. The complex ray model assumes the probe beam to be a bundle of rays that propagate in a complex space. In the field of thermal wave, the ray trajectory is changed as a consequence of its optical path change resulting from the change in the gas refractive index and the change in the refractive index gradient. These let us take into account the deflection and the phase change of the probe beam in the field of thermal wave.

In this work, a method of determining thermal parameters of solid samples, by the use of complex geometrical optics equations, is presented. The measurement method is based on the mirage effect and the experimental data are analyzed using four parameters least-squares regression fitting for the theoretical curves calculated on the basis of CRM. The analysis is also performed for GOM and WOM and results are compared to those received in the framework of complex geometrical optics.

2. Thermal field

The steady-state temperature field distribution in gas above a flat, thermally homogeneous and isotropic sample with thickness d, produced by a modulated light beam that heats its surface uniformly, is [14–16]:

$$\vartheta_g(x, t) = a_g + b_g \exp(-k_g x)\cos(\Omega t - k_g x + \varphi_g) \tag{1a}$$

where

$$a_g = q_0 \frac{d}{\lambda_s} \tag{1b}$$

$$b_g = \theta_g \exp(-k_g h) \tag{1c}$$

$$\varphi_g = \gamma_g - k_g h \tag{1d}$$

$$\theta_g = \frac{q_0 G \exp(k_s d)}{2\left[\exp(4k_s d)p^2 + 2pr\exp(2k_s d)\cos(2k_s d) + r^2\right]} X Y \tag{1e}$$

$$X = \sqrt{\exp(2k_s d) + \exp(-2k_s d) - 2\cos(2k_s d)}$$

$$Y = \sqrt{\left[\exp(2k_s d)pu + rw\right]^2 + \left[\exp(2k_s d)pw + ru\right]^2}$$

$$\gamma_g = -\operatorname{atan}\left[\frac{\exp(k_s d) + \exp(-k_s d)}{\exp(k_s d) - \exp(-k_s d)}\tan(k_s d)\right] - \operatorname{atan}\left[\frac{\exp(2k_s d)pw + ru}{\exp(2k_s d)pu + rw}\right] \tag{1f}$$

$$p = k_g \lambda_g + k_s \lambda_s \tag{1g}$$

$$r = k_s \lambda_s - k_g \lambda_g \tag{1h}$$

$$u = \cos(k_s d) - \sin(k_s d) \tag{1i}$$

$$w = \cos(k_s d) + \sin(k_s d) \tag{1j}$$

Here a_g is the constant rise of the temperature in gas, b_g is the amplitude of the harmonic component of the sample surface temperature, φ_g is the phase shift between the sample surface temperature and the pump beam. The time-dependent part of the solution (1a)

represents the so-called one-dimensional thermal waves, in which $k_g = \sqrt{\Omega / 2\kappa_g}$ and $k_s = \sqrt{\Omega / 2\kappa_s}$ are the wave number of these waves in the gas and the sample, respectively, κ_g and κ_s are thermal diffusivities of the gas and the sample, λ_g and λ_s are their thermal conductivities, q_0 is the energy flux that incidents on the sample surface. The Eqs. (1b)–(1j) describe the situation in which the lower side of the sample ($x = -d$) is kept at the ambient temperature.

3. The propagation of the Gaussian probe beam in the thermally disturbed medium

As a result of the probe beam interaction with the field of thermal wave, the light intensity distribution in it is changed. The changes in the probe beam light intensity are usually registered by the use of quadrant photodiode [3–6], what results in the photodeflection signal which can be calculated as [3–8]:

$$S_n = K_d \int_{-\infty}^{+\infty} \mathrm{d}y_D \left(\int_{0}^{+\infty} - \int_{-h}^{0} \right) \mathrm{d}x_D \, I(\mathbf{r_D}) = A_i \cos(\Omega t + \varphi_g + \varphi_i) \tag{2}$$

where K_d is the photodetector constant, h is the height of the probe beam over the sample, $I(\mathbf{r_D})$ is the probe beam light intensity in the detector plane, A_i is the amplitude of the photodeflection signal, φ_i is the phase of it depending on the theoretical model used ($i = C$ for the CRM, $i = G$ for the GOM, $i = W$ for the WOM).

All the theories of the photodeflection signal formation try to find the probe beam light intensity after undergoing the thermal lens $I(\mathbf{r})$ using different tools. As the result of these theoretical calculations, the quantities A_i and φ_i are functions of many parameters of the experimental setup as well as the thermal and geometrical parameters of the sample. For the assumed detection geometry (Fig. 1) the set of these parameters contains the height of the probe beam over the sample h, the angular modulation frequency Ω, the probe beam radius a, the beam waist position L, the detector z_D and the sample z_l positions, the sample thermal conductivity λ_s, its thermal diffusivity κ_s and its thickness d.

It should be noticed that not all parameters, mentioned above, were taken into account in works about GOM and WOM or they described experimental setups different from ours by some details. That is why it was necessary to recalculate the photodeflection signal on the basis of (2) for both models. The received results are presented in Appendix B and C.

3.1. The complex geometrical optics model (CRM)

The complex ray model (CRM) assumes the probe beam (the Gaussian one) to be a bundle of rays that propagate in a 6D complex space. Thus, each of these rays is described by a set of equations called the ray trajectory [8–13, 17]. In the thermally disturbed medium the probe beam interacts with the thermal lens and as a result of that

it is deflected. Deflection means the change of the ray trajectory. The ray trajectory change results in changing the amplitude of the electric field in the probe beam [8–13, 17]. The probe beam propagation in optically nonhomogeneous medium results also in its phase change caused by the change of the optical path of the ray (resulting from deflection which causes the change of the geometrical path of the ray and the change of the gas refractive index in the field of thermal wave). The correction to the x coordinate of the ray and to the eikonal (a function describing the optical path of the ray) is found on the grounds of the perturbation calculus [17]. It should be remembered that the correction of the amplitude of the beam and its eikonal are complex. It means that both of them influence the value of the amplitude and the phase of the light beam intensity [8–13].

The photodeflection signal depends on λ_s and κ_s because of the amplitude of the sample surface temperature b_g and the phase shift between the sample surface temperature and the pump beam φ_g depending on them. That is why the formulas describing its amplitude and phase can be written as a function of b_g and φ_g [8–13] (see Appendix A):

$$A_C = b_g N_C(a, h, L, \Omega, z_D, z_l) \tag{3}$$

$$\varphi_C = \Lambda_C(a, h, L, \Omega, z_D, z_l) + \varphi_g \tag{4}$$

where the normalizing factor $N_C(a, h, L, \Omega, z_D, z_l)$ and the part of the phase change $\Lambda_C(a, h, L, \Omega, z_D, z_l)$, both independent of b_g and φ_g, are expressed by rather complicated analytical formulas shown elsewhere [8–13].

3.2. The geometrical optics model (GOM)

This model considers the probe beam to be a bundle of rays. Each of them is deflected on the thermal lens proportionally to the temperature gradient in it. The photodeflection signal is obtained by averaging their contribution in accordance with the undisturbed probe beam intensity profile.

The amplitude A_G of the photodeflection signal received in this case can be also written as a product of the amplitude of the sample surface temperature b_g and the normalizing factor $N_G(a, h, L, \Omega, z_D, z_l)$ independent of b_g (see Appendix B):

$$A_G = b_g N_G(a, h, L, \Omega, z_D, z_l) \tag{5}$$

whereas its phase φ_G is a sum of two components:

$$\varphi_G = \Lambda_G(a, h, L, \Omega, z_D, z_l) + \varphi_g \tag{6}$$

First of them is not a function of thermal parameters of the sample, while the second one is equal to the phase shift between the sample surface temperature and the pump beam φ_g and depends on λ_s, κ_s and d [8–13].

3.3. The wave optics model (WOM)

The idea of the wave theory is based on the thin lens approximation of the temperature field in gas above the sample. Such assumption means that only the phase changes in the electric field of the probe beam caused by its interaction with the field of thermal wave are taken into account. Distortions of the amplitude distribution resulting from the deflection on the refractive index gradients are out of interest in this theory. In case of WOM, as in previous models, the photodeflection signal amplitude and phase are described by (see Appendix C):

$$A_W = b_g N_W(a, h, L, \Omega, z_D, z_l) \tag{7}$$

$$\varphi_W = \Lambda_W(a, h, L, \Omega, z_D, z_l) + \varphi_g \tag{8}$$

It is seen from Eqs. (3)–(8) that in all cases the amplitudes and phases of the photodeflection signal differ from each other only by the setup factors depending on the parameters of an experimental setup. All information about sample thermal parameters are included only in b_g and φ_g factors. In the experiment we are able to measure quantities A_i and φ_i, so the correct determination of b_g and φ_g factors is possible when the correct values of these setup factors N_i and Λ_i are known.

4. Experimental results

In the experiments, the typical photodeflection setup was used. A laser diode with the output wavelength of λ_e = 830 nm was used as a pump beam source. The pump beam light was modulated by its turning on and off. A helium-neon laser (λ = 633 nm) was used as a probe beam source. It provides a Gaussian beam.

A sample with known thermal properties was selected to test this method with air as a deflecting medium. The zinc plate of 0.5 mm thickness was used in the experiments. The thermal diffusivity was determined using a four parameter least-squares-fitting of the normal photodeflection signal amplitude and phase versus the angular modulation

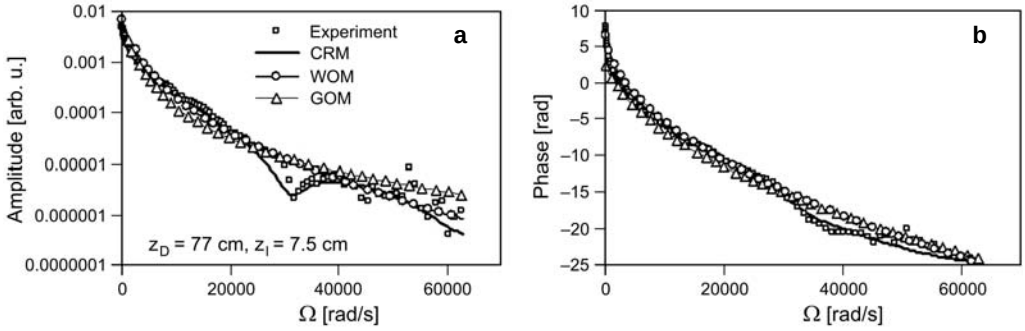

Fig. 2. The amplitude (**a**) and the phase (**b**) of photodeflection signal changes versus modulation frequencies of temperature field Ω.

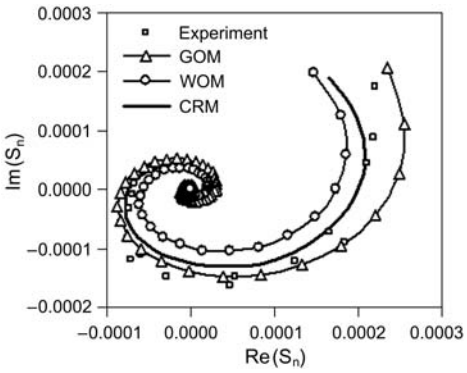

Fig. 3. Argand's graph for the data presented in Fig. 2. $\mathrm{Re}(S_n)$ and $\mathrm{Im}(S_n)$ are respectively the real and imaginary parts of the normal component of the photodeflection signal.

T a b l e. Received values of thermal and experimental setup parameters determined on the basis of CRM, WOM and GOM

Material and tabulated thermal parameters [15]	Model	Values of determined parameters			
		κ_s [m^2/s]	a [μm]	L [cm]	h [μm]
zinc ($\kappa_s = 4.18\times10^{-5}$ m^2/s, $\lambda_s = 116$ W/mK)	CRM	4.42×10^{-5}	109	7.8	200
	WOM	3.57×10^{-5}	115	7.5	200
	GOM	2.44×10^{-5}	125	8.6	180

frequency of the temperature field Ω (Fig. 2) for the thermal diffusivity κ_s of a sample, the probe beam radius a, its waist position L and the height of the probe beam over the sample h. To be able to fit both the amplitude and the phase of the signal, the least--square procedure was performed for the Argand's graph (Fig. 3). Additionally, the fitting was performed for such range of experimental setup parameters changes that the experimental data are well described only by CRM (Fig. 2).

Figure 2 presents the photodeflection signal amplitude and phase changes as functions of the angular modulation frequency of the excitation radiation Ω. It can be seen from it that the amplitude not always decreases with the increase of Ω. There are some frequency ranges in which an increase in signal amplitude is observed. This behavior cannot be reproduced neither by the geometrical nor wave optics models but can be reproduced within a complex ray model. The observed effect arises from the fact that with the increase of frequency, the thermal wave attenuation increases. But the temperature field gradient also increases. These two competitive processes can mean that the amplitude of the photothermal signal does not decrease monotonously with the increase of Ω, but there are some frequencies ranges in which the second effect overbalances and the signal increases.

The results of the fitting, the values of obtained thermal parameters of the examined sample and the parameters of an experimental setup are presented in the Table.

The least-squares method applied with calculations in the GOM and WOM yield a value of the thermal diffusivity differing by more than ten percents from the literature value. Calculations with the CRM give a more accurate value of the thermal parameters of this sample.

In case of the experimental setup parameters determination, the differences between the received values of a, h and L for all theories are about ten percents. It means that the kind of a theoretical approach (GOM, WOM or CRM) used in the fitting stronger influences the sample thermal parameters determination than the experimental setup ones.

5. Conclusions

In the paper, the determination of thermal parameters of a zinc sample on the basis of GOM, WOM and CRM was carried out.

The photodeflection signal depends on the thermal parameters of the sample because the temperature on its surface is a function of those parameters. It can be seen from Eqs. (3)–(8) that in all cases the signal amplitudes are proportional to the temperature of the sample's surface b_g and differ from each other only by the factor depending on the parameters of an experimental setup. Moreover, their phases consist of two components – one of them is independent of κ_s and λ_s, while the second one is equal to the phase shift between the sample's surface temperature and the pump beam φ_g.

There was shown in [2, 18–21] that the use of a geometrical optics approach for determining the thermal parameters of samples often leads to errors, especially in the case of measurements when high modulation frequencies of temperature field are needed or a large probe beam radius is required, and also when the thermal diffusivity, that needs to be determined, is small compared to that of the deflecting medium. It means that the factor N_i ($i = C$ for CRM, $i = G$ for GOM, $i = W$ for WOM) in Eqs. (3), (5), (7) and the part of the phase change Λ_i independent of κ_s and λ_s influences the correctness of determining the thermal parameters of different kinds of the samples. In this work it has been proved that the complex ray model should be used for determining those parameters because it gives more accurate values (the Table). It means that the CRT gives both the correct qualitative and quantities interpretation of the experimental data.

Appendix A

The quantities N_C and Λ_C are described by:

$$N_C = \sqrt{A_{do}^2 + A_{fo}^2 + 2A_{do}A_{fo}(\cos\varphi_d \cos\varphi_f - \sin\varphi_d \sin\varphi_f)} \tag{A1}$$

$$\Lambda_C = \operatorname{atan}\frac{A_{do}\sin\varphi_d - A_{fo}\sin\varphi_f}{A_{do}\cos\varphi_d + A_{fo}\cos\varphi_f} \tag{A2}$$

where

$$A_{fo} = \frac{1}{2}K_d n_0 s_T k I_m(z_p - z_l)\sqrt{(\operatorname{Im}F_1 + \operatorname{Im}F_2)^2 + (\operatorname{Re}F_2 - \operatorname{Re}F_1)^2} \tag{A3}$$

$$A_{do} = \sqrt{\left[A_{dAo}\cos\varphi_{dA} + A_{dfo}\cos\left(\varphi_{df} - \frac{\pi}{4}\right)\right]^2 + \left[A_{dAo}\sin\varphi_{dA} + A_{dfo}\sin\left(\varphi_{df} - \frac{\pi}{4}\right)\right]^2} \tag{A4}$$

$$A_{dAo} = iK_d s_T k_g C_x I_m \sqrt{\frac{\pi}{f}} \frac{(z_D - z_s)(z_p - z_l)}{1 + i\dfrac{z_D}{z_{RC}}} \sqrt{(\mathrm{Re}G_1 - \mathrm{Re}G_2)^2 + (\mathrm{Im}G_1 + \mathrm{Im}G_2)^2} \tag{A5}$$

$$A_{dfo} = -i\sqrt{2}\, K_d I_m k s_T k_g z_D n_0 \frac{(z_D - z_s)(z_p - z_l)}{z_{RC}^2\left(1 + i\dfrac{z_D}{z_{RC}}\right)^2} \sqrt{(\mathrm{Re}H_1 + \mathrm{Re}H_2)^2 + (\mathrm{Im}H_1 - \mathrm{Im}H_2)^2} \tag{A6}$$

$$\varphi_{dA} = -\mathrm{atan}\frac{\mathrm{Im}(G_1 + G_2)}{\mathrm{Re}(G_1 - G_2)} \tag{A7}$$

$$\varphi_{df} = -\mathrm{atan}\frac{\mathrm{Re}(H_1 + H_2)}{\mathrm{Im}(H_1 - H_2)} \tag{A8}$$

$$F_1 = \exp\left[\left(\frac{(1+i)C_x}{2\sqrt{f}}\right)^2\right]\left[1 - 2\mathrm{erf}\left(\frac{(1+i)C_x}{2\sqrt{f}}\right) + \mathrm{erf}\left(\frac{(1+i)C_x}{2\sqrt{f}} - h\sqrt{f}\right)\right] \tag{A9}$$

$$F_2 = \exp\left[\left(\frac{(1-i)C_x}{2\sqrt{f}}\right)^2\right]\left[1 - 2\mathrm{erf}\left(\frac{(1-i)C_x}{2\sqrt{f}}\right) + \mathrm{erf}\left(\frac{(1-i)C_x}{2\sqrt{f}} - h\sqrt{f}\right)\right] \tag{A10}$$

$$G_1 = \exp\left[(i-1)^2\frac{C_x^2}{4f}\right]\left\{\mathrm{erf}\left[\frac{(i-1)C_x}{2\sqrt{f}}\right] - \frac{1}{2}\mathrm{erf}\left[\frac{(i-1)C_x}{2\sqrt{f}} + h\sqrt{f}\right] + \frac{1}{2}\right\} \tag{A11}$$

$$G_2 = \exp\left[(i+1)^2\frac{C_x^2}{4f}\right]\left\{\mathrm{erf}\left[\frac{-(i+1)C_x}{2\sqrt{f}}\right] - \frac{1}{2}\mathrm{erf}\left[\frac{-(i+1)C_x}{2\sqrt{f}} + h\sqrt{f}\right] + \frac{1}{2}\right\} \tag{A12}$$

$$H_1 = \left\{\frac{\sqrt{\pi}\,(i-1)C_x}{4f^{3/2}}\exp\left[\frac{(i-1)^2C_x^2}{4f}\right]\left[\mathrm{erf}\left(\frac{(i-1)C_x}{2\sqrt{f}} + h\sqrt{f}\right) - \mathrm{erf}\left(\frac{(i-1)C_x}{2\sqrt{f}}\right)\right]\right.$$
$$\left. + \frac{1}{2f}\exp\left[-(i-1)C_x h - fh^2\right] - \frac{\sqrt{\pi}\,(i+1)C_x}{4f^{3/2}}\exp\left[\frac{(i+1)^2C_x^2}{4f}\right]\left[1 - \mathrm{erf}\left(\frac{(i+1)C_x}{2\sqrt{f}}\right)\right]\right\} \tag{A13}$$

$$H_2 = \left\{ \frac{\sqrt{\pi}\,(i-1)C_x}{4f^{3/2}} \exp\left[\frac{(i-1)^2 C_x^2}{4f}\right]\left[1 - \operatorname{erf}\left(\frac{-(i-1)C_x}{2\sqrt{f}}\right)\right] + \frac{1}{2f}\exp\left[(i+1)C_x h - f h^2\right] + \frac{\sqrt{\pi}\,(i+1)C_x}{4f^{3/2}} \exp\left[\frac{(i+1)^2 C_x^2}{4f}\right]\left[\operatorname{erf}\left(\frac{-(i+1)C_x}{2\sqrt{f}}\right) - \operatorname{erf}\left(\frac{-(i+1)C_x}{2\sqrt{f}} + h\sqrt{f}\right)\right]\right\} \tag{A14}$$

$$C_x = k_g\left(1 + i\frac{z_s}{z_{RC}}\right)\left(1 + i\frac{z_D}{z_{RC}}\right)^{-1} \tag{A15}$$

$$I_m = \frac{z_R P_l}{\sqrt{\pi}\; a\sqrt{z_R^2 + (L - z_D)^2}} \tag{A16}$$

$$f = \frac{z_R^2}{a^2\left[z_R^2 + (L - z_D)^2\right]} \tag{A17}$$

and erf(ξ) is the error function, P_l is the total power of an undisturbed probe beam, $z_R = ka^2 n_0$ is the Rayleigh length, $z_{RC} = z_R - iL$ is the complex Rayleigh length.

Appendix B

The normalizing factor N_G and the part of the phase shift Λ_G independent of thermal and geometrical parameters of the sample received on the grounds of the geometrical optics model are expressed by:

$$N_G = \sqrt{(\operatorname{Re} P_1 + \operatorname{Re} P_2)^2 + (\operatorname{Im} P_1 + \operatorname{Im} P_2)^2} \tag{B1}$$

$$\Lambda_G = \operatorname{atan}\left(-\frac{\operatorname{Im} P_1 + \operatorname{Im} P_2}{\operatorname{Re} P_1 - \operatorname{Re} P_2}\right) + \frac{\pi}{4} \tag{B2}$$

$$P_1 = -i\,\frac{\sqrt{2}}{2}\,\pi K_d a^2 s_T k_g (z_p - z_l)\exp\left\{\frac{a^2}{4}\left[(1+i)k_g\right]^2\right\} \times\left\{1 - 2\operatorname{erf}\left[\frac{a(1+i)k_g}{2}\right] - \operatorname{erf}\left[\frac{h}{a} - \frac{a(1+i)k_g}{2}\right]\right\} \tag{B3}$$

$$P_2 = -i\,\frac{\sqrt{2}}{2}\,\pi K_d a^2 s_T k_g (z_p - z_l)\exp\left\{\frac{a^2}{4}\left[(1-i)k_g\right]^2\right\} \times\left\{1 + 2\operatorname{erf}\left[\frac{a(1-i)k_g}{2}\right] - \operatorname{erf}\left[\frac{h}{a} - \frac{a(1-i)k_g}{2}\right]\right\} \tag{B4}$$

Appendix C

The N_W and Λ_W can be written in a form:

$$N_w = \sqrt{\left[\mathrm{Re}\left(\sum_{i=1}^{4} T_i\right)\right]^2 + \left[\mathrm{Im}\left(\sum_{i=3}^{4} T_i - \sum_{i=1}^{2} T_i\right)\right]^2} \tag{C1}$$

$$\Lambda_w = \mathrm{atan}\frac{\mathrm{Im}\left(\sum_{i=1}^{2} T_i\right) - \mathrm{Im}\left(\sum_{i=3}^{4} T_i\right)}{\mathrm{Re}\left(\sum_{i=1}^{4} T_i\right)} \tag{C2}$$

$$\begin{aligned} T_1 = {} & \frac{\pi\sigma_m R_\alpha}{2\sqrt{R_1 R_2}}\left\{(\delta_0 + i\delta_1)\cos\left[k(z_l - L)\right] - (\delta_1 - i\delta_0)\sin\left[k(z_l - L)\right]\right\} \\ & \times \exp\left[-k_g^2 a^2(\alpha_1 - i\alpha_2) - ik(z_l - L) - k_g^2 k^2 \frac{a^4}{4}(\alpha_1 - i\alpha_2)^2 (z_D - z_s)^{-2} R_1^{-1}\right] \\ & \times \left\{1 - \mathrm{erf}\left[-i\sqrt{R_1}\,h + ik_g k \frac{a^2}{2}(\alpha_1 - i\alpha_2)(z_D - z_s)^{-1}\sqrt{R_1^{-1}}\right]\right\} \end{aligned} \tag{C3}$$

$$\begin{aligned} T_2 = {} & \frac{\pi\sigma_m R_\beta}{2\sqrt{R_4 R_2}}\left\{(\delta_0 - i\delta_1)\cos\left[k(z_l - L)\right] - (\delta_1 + i\delta_0)\sin\left[k(z_l - L)\right]\right\} \\ & \times \exp\left[k_g^2 a^2(\alpha_3 - i\alpha_4) - ik(z_l - L) - k_g^2 k^2 \frac{a^4}{4}(\alpha_3 - i\alpha_4)^2 (z_D - z_s)^{-2} R_4^{-1}\right] \\ & \times \left\{1 - \mathrm{erf}\left[-i\sqrt{R_4}\,h - ik_g k \frac{a^2}{2}(\alpha_3 - i\alpha_4)(z_D - z_s)^{-1}\sqrt{R_4^{-1}}\right]\right\} \end{aligned} \tag{C4}$$

$$\begin{aligned} T_3 = {} & \frac{\pi\sigma_m R_\alpha}{2\sqrt{R_3 R_2}}\left\{(\delta_0 + i\delta_1)\cos\left[k(z_l - L)\right] - (\delta_1 - i\delta_0)\sin\left[k(z_l - L)\right]\right\} \\ & \times \exp\left[k_g^2 a^2(\alpha_3 + i\alpha_4) - ik(z_l - L) - k_g^2 k^2 \frac{a^4}{4}(\alpha_3 + i\alpha_4)^2 (z_D - z_s)^{-2} R_3^{-1}\right] \\ & \times \left\{1 - \mathrm{erf}\left[-i\sqrt{R_3}\,h - ik_g k \frac{a^2}{2}(\alpha_3 + i\alpha_4)(z_D - z_s)^{-1}\sqrt{R_3^{-1}}\right]\right\} \end{aligned} \tag{C5}$$

$$T_4 = \frac{\pi\sigma_m R_\beta}{2\sqrt{R_5 R_2}}\left\{(\delta_0 - i\delta_1)\cos\left[k(z_l - L)\right] - (\delta_1 + i\delta_0)\sin\left[k(z_l - L)\right]\right\}$$
$$\times \exp\left[-k_g^2 a^2(\alpha_1 + i\alpha_2) - ik(z_l - L) - k_g^2 k^2 \frac{a^4}{4}(\alpha_1 + i\alpha_2)^2 (z_D - z_s)^{-2} R_5^{-1}\right]$$
$$\times\left\{1 - \mathrm{erf}\left[-i\sqrt{R_5}\,h + ik_g k\frac{a^2}{2}(\alpha_1 + i\alpha_2)(z_D - z_s)^{-1}\sqrt{R_5^{-1}}\right]\right\} \tag{C6}$$

$$\sigma_m = \frac{s_T k^2 P_l z_R^4}{4n_0^2 a^2 \pi^3}\frac{(z_l - L - iz_R)(z_p - z_l)}{(z_D - z_s)^3 (z_l^2 + z_R^2)}\left[z_R^2 + L^2 - 3(z_R^2 + L^2)^{-1} z_l^2 L^2 + (z_R^2 + L^2)^{-3} z_l^4 L^4\right]^{-1}$$
$$\times\left[1 + \left(\frac{z_l - L}{z_R}\right)^2\right]^2\left\{1 - \left[\frac{k}{2}(z_D - z_s)^{-1}\left[1 + \left(\frac{z_l - L}{z_R}\right)^2\right] - 2\frac{z_l - L}{kn_0}\right]^2\right\}^{-1} \tag{C7}$$

$$\delta_0 = \frac{(z_R^2 + L^2)^2}{(z_R^2 + L^2 - z_l L)^2 + z_R^2 z_l^2}\times\left\{\frac{2z_R(z_D - z_s)}{k}\left[1 + \frac{(z_l - L)^2}{z_R^2}\right]\left(1 - 2\frac{z_l L}{z_R^2 + L^2}\right)\right.$$
$$\left. + \frac{kn_0}{2z_R}(z_l - L)\left[1 + \frac{(z_l - L)^2}{z_R^2}\right]^{-1}\right\} \tag{C8}$$

$$\delta_1 = \frac{k}{2}\left[1 + \left(\frac{z_l - L}{z_R}\right)^2\right]^{-1}\left[(z_D - z_s)^{-1} - \frac{n_0}{z_R^2}(z_l - L)^2 + n_0\frac{(z_R^2 + L^2)^2}{(z_R^2 + L^2 - z_l L)^2 + z_R^2 z_l^2}\right] \tag{C9}$$

$$R_1 = -\frac{k}{z_D - z_s}\left\{(z_D - z_s)^{-1}\left[\frac{z_R}{2n_0} + ka^2(i\alpha_2 - \alpha_1)\right] + \frac{i}{2}\left[1 + \frac{z_l - L}{z_R}\right]\right\} \tag{C10}$$

$$R_2 = -\frac{k}{2(z_D - z_s)}\left\{\frac{z_R}{n_0(z_D - z_s)} - i\left[1 + \frac{z_l - L}{z_R}\right]\right\} \tag{C11}$$

$$R_3 = -\frac{k}{z_D - z_s}\left\{(z_D - z_s)^{-1}\left[\frac{z_R}{2n_0} + ka^2(\alpha_4 + i\alpha_3)\right] - \frac{i}{2}\left[1 + \frac{z_l - L}{z_R}\right]\right\} \tag{C12}$$

$$R_4 = -\frac{k}{z_D - z_s}\left\{(z_D - z_s)^{-1}\left[\frac{z_R}{2n_0} + ka^2(\alpha_4 - i\alpha_3)\right] - \frac{i}{2}\left[1 + \frac{z_l - L}{z_R}\right]\right\} \tag{C13}$$

$$R_5 = -\frac{k}{z_D - z_s}\left\{(z_D - z_s)^{-1}\left[\frac{z_R}{2n_0} + ka^2(\alpha_1 + i\alpha_2)\right] - \frac{i}{2}\left[1 + \frac{z_l - L}{z_R}\right]\right\} \tag{C14}$$

$$\alpha_1 = \frac{1}{2}\left[1 + \left(\frac{z_l - L}{z_R}\right)^2\right]\left\{1 - \left[\frac{z_R}{n_0(z_D - z_s)}\left[1 + \left(\frac{z_l - L}{z_R}\right)^2\right] - \frac{z_l - L}{z_R}\right]^2\right\}^{-1} \tag{C15}$$

$$\alpha_2 = \alpha_1\left\{\frac{z_R}{n_0(z_D - z_s)} - \left[1 + \left(\frac{z_l - L}{z_R}\right)^2\right]^{-1}\right\} \tag{C16}$$

$$\alpha_3 = \frac{1}{2}\left[1 - \left(\frac{z_l - L}{z_R}\right)^2\right]\left\{1 - \left[\frac{z_R}{n_0(z_D - z_s)}\left[1 - \left(\frac{z_l - L}{z_R}\right)^2\right] - \frac{z_l - L}{z_R}\right]^2\right\}^{-1} \tag{C17}$$

$$\alpha_4 = \alpha_3\left[1 - \left(\frac{z_l - L}{z_R}\right)^2\right]\left\{\frac{z_R}{n_0(z_D - z_s)} - \left[1 - \left(\frac{z_l - L}{z_R}\right)^2\right]^{-1}\right\} \tag{C18}$$

References

[1] SALAZAR A., SANCHEZ-LAVEGA A., FERNANDEZ J., *Theory of thermal diffusivity determination by the 'mirage' technique in solids*, Journal of Applied Physics **65**(11), 1989, pp. 4150–6.

[2] GLAZOV A.L., MURATIKOV K.L., *Measurement of thermal parameters of solids by a modified photodeflection method*, Optical Engineering **36**(2), 1997, pp. 358–62.

[3] AAMODT L.C., MURPHY J.C., *Photothermal measurements using a localized excitation source*, Journal of Applied Physics **52**(8), 1981, pp. 4903–14.

[4] LEGAL LASALLE E., LEPOUTRE F., ROGER J.P., *Probe beam size effects in photothermal deflection experiments*, Journal of Applied Physics **64**(1), 1988, pp. 1–5.

[5] JIANHUA ZHAO, JUN SHEN, CHENG HU., *Continuous-wave photothermal deflection spectroscopy with fundamental and harmonic responses*, Optics Letters **27**(20), 2002, pp. 1755–7.

[6] ROHLING J.H., JUN SHEN, JIANQIN ZHOU, GU C.E., MEDINA A.N., BAESSO-ML., *Application of the diffraction theory for photothermal deflection to the measurement of the temperature coefficient of the refractive index of a binary gas mixture*, Journal of Applied Physics **99**(10), 2006, p. 103107.

[7] LI B., XIONG S., ZHANG Y., *Fresnel diffraction model for mode-mismatched thermal lens with top-hat beam excitation*, Applied Physics B: Lasers and Optics **80**(4–5), 2005, pp. 527–34.
[8] KORTE KOBYLIŃSKA D., BUKOWSKI R.J., BURAK B., BODZENTA J., KOCHOWSKI S., *Photodeflection signal formation in photothermal measurements: comparison of the complex ray theory, the ray theory, the wave theory, and experimental results*, Applied Optics **46**(22), 2007, pp. 5216–27.
[9] KORTE KOBYLIŃSKA D., BUKOWSKI R.J., BURAK B., BODZENTA J., KOCHOWSKI S., *The complex ray theory of photodeflection signal formation: comparison with the ray theory and the experimental results*, Journal of Applied Physics **100**(6), 2006, p. 63501.
[10] BUKOWSKI R.J., KORTE D., *Perturbation calculus for eikonal application to analysis of the deflectional signal in photothermal measurements*, Optica Applicata **32**(4), 2002, pp. 817–28.
[11] BUKOWSKI R.J., KORTE D., *Influence of probing beam focusing on photothermal signal*, Journal de Physique IV: Proceedings **109**, 2003, pp. 19–31.
[12] BUKOWSKI R.J., KORTE D., *Deflective signal analysis in photothermal measurements in the frame of complex geometrical optics*, Optica Applicata **35**(1), 2005, pp. 77–97.
[13] KOBYLIŃSKA D., BUKOWSKI R.J., BURAK B., KOCHOWSKI S., *Gaussian optical beam propagation in thermal wave field – ray theory, the complex ray theory and experimental results*, Journal de Physique IV: Proceedings **129**, 2005, pp. 231–6.
[14] BUKOWSKI R.J., *Geometrical optics application in description of gaussian beam propagation in an optically homogenous medium*, Proceedings of the 2nd National Conference Physical Basis of the Nondestructive Investigations, Gliwice Chapter of the Polish Physical Society and Institute of Physics of the Silesian University of Technology, Gliwice'97 (in Polish).
[15] BODZENTA J., *Thermal wave in photothermal measurements of solid states*, Zeszyty Naukowe Politechniki Śląskiej, Seria: Matematyka – Fizyka, z. 85, 1999 (in Polish).
[16] CARSLAW H.S., JAEGER J.C., *Conduction of Heat in Solids*, Oxford University Press, Oxford 1959.
[17] KRAVTSOV JU.A., ORLOV JU.I., *Geometrical Optics of the Nonhomogeneous Media*, WNT, Warsaw 1993 (in Polish).
[18] GLAZOV A.L., MURATIKOV K.L., *Photodeflection signal formation in thermal wave spectroscopy and microscopy of solids within the framework of wave optics. 'Mirage' effect geometry*, Optics Communications **84**(5–6), 1991, pp. 283–9.
[19] MURATIKOV K.L., GLAZOV A.L., *Measurement of thermophysical parameters of bulk materials by a photodeflection method*, Technical Physics Letters **21**(11), 1995, pp. 876–8.
[20] MURATIKOV K.L., GLAZOV A.L., WALTHER H.G., *Photothermal measurement of the thermal parameters of volume materials and thin films by the photodeflection method*, High Temperatures – High Pressures **31**(1), 1999, pp. 69–73.
[21] WALTHER H.G., MURATIKOV K.L., GLAZOV A.L., *Thermal diffusivity determination by the photodeflection method. The influence of wave optical effects*, Journal de Physique IV: Colloque **4**(C7), 1994, pp. C7/291–4.

Received October 2, 2007
in revised form December 5, 2007